

## Drying-generated stresses of non saturated hardened cement paste under variable conditions

Ben Abdelhamid Manel <sup>1</sup>, Mihoubi Daoued <sup>2</sup>, Sghaier Jalila <sup>3</sup>, Bellagi Ahmed<sup>4</sup>

<sup>1</sup>Unité de Recherche de Thermique et Thermodynamique des Procédés Industriels

Département de Génie Energétique, Ecole Nationale d'Ingénieurs de Monastir

Avenue Ibn Eljazzar, 5019 Monastir, Tunisie

[benabdelhamidmanel@yahoo.fr](mailto:benabdelhamidmanel@yahoo.fr)

<sup>2</sup>Laboratoire des Procédés Thermiques, CRTEN

B.P. 95, 2050 Hammam-Lif, Tunisie

[daoued.mihoubi@crtten.rnrt.tn](mailto:daoued.mihoubi@crtten.rnrt.tn)

**Abstract:** In this work, a comparative analysis of the behaviour of hardened cement paste during drying at constant and variable conditions is presented. A multiphase mathematical model based on averaged theory was developed to describe the coupled heat, mass and momentum transfers within non saturated porous media. In this approach, only the elastic behaviour of the medium through Hooke's law was considered. Drying under variable conditions consisted in periodical changes of drying air parameters (temperature, relative humidity and combined temperature and relative humidity). The drying kinetics and the mechanical behaviour were examined in terms of moisture content, temperature, gas pressure, water saturation and induced stresses. It was observed that drying with periodical variation of air temperature combined with relative humidity changes produces the lowest stresses within the material without extending the drying time.

**Keywords:** Hardened cement paste, drying kinetics, stress, air conditions, saturation

### 1 Introduction

Cement-based materials are generally subjected to thermo-hydric gradient. The drying process brings a coupled water transport and induced mechanical stresses that affect stability of material. Indeed, as a consequence of non uniform humidity distribution within the material a volumetric shrinkage and stresses development

are generated [1,2]. For this purpose, several modelling approaches were developed in order to take into account the thermo-hydro mechanical frameworks e.g., the diffusion theory, the capillary-porous theory, the evaporation-condensation theory, etc [3,4,5,6]. The development of generated stresses implies usually the risk of material crack and quality deterioration. One of the latest methods used to moderate stresses growth is drying at variable air conditions such air temperature and relative humidity. This technique consists in reducing periodically the evaporation rate to make moisture homogeneity [7,8]. A good management of external conditions is indispensable to provide a better quality of material without affecting drying time [9].

This paper focuses mainly on the thermo-hydro-mechanical model taking into account the presence of three fluid phases (liquid water, vapour and dry air). This approach is based on volume-averaged conservation equations in porous media. The state variables retained in the model are the saturation  $S_i$ , the porosity  $\phi$ , the gas pressure  $\langle P_g \rangle^g$ , the temperature  $T$  and the solid velocity  $\langle \vec{V}_s \rangle^s$ . The first part of the paper consists of a presentation of the coupled equation system for non saturated elastic porous media. In the next section we present a comparison of the material behaviour during drying under constant and variable conditions. In fact, the porous structure of hardened cement paste is subjected to periodical alterations of air temperature, air relative humidity and combined variation of air temperature and relative humidity. The efficiency of this method of drying was examined in terms of quality of dried materials and drying kinetics.

## 2 Mathematical model

A hardened cement paste sample is considered as an isotropic elastic porous media composed of three phases: solid, liquid and gas (vapour and dry air). A hydro-thermo-mechanical model based on volume averaging theory [3] for deformable media was developed to describe the material behaviour during drying. The mathematical model consists of the heat and mass conservation equations system coupled with conservation momentum equation via the effective stress theory of Terzaghi. Darcy's law is used to describe moisture flow into sample. Fick's law is related to vapour and dry air phases for diffusive aspects. Local thermal equilibrium between phases is maintained and the model is applied in two-dimensional configurations.

### 2.1 Mass conservation equations

The equations system describing the drying process is the following:

The mass conservation in the solid skeleton:

$$\frac{\partial \langle \rho_s \rangle}{\partial t} + \text{div}(\langle \rho_s \rangle \langle \vec{V}_s \rangle^s) = 0 \quad (1)$$

In which  $\langle \rho_s \rangle = \langle \rho_s \rangle^s (1 - \phi)$

The solid skeleton is considered as incompressible,  $\langle \rho_s \rangle^s$  is constant,

$$-\frac{\partial \phi}{\partial \tau} + \text{div} \left( (1 - \phi) \langle \vec{V}_s \rangle^s \right) = 0 \quad (2)$$

The mass conservation equations in the liquid, vapour and dry air phases are:

$$\frac{\partial \langle \rho_l \rangle}{\partial \tau} + \text{div}(\langle \rho_l \rangle \langle \vec{V}_l \rangle^l) = -\dot{m}_v \quad (3)$$

$$\frac{\partial \langle \rho_v \rangle}{\partial \tau} + \text{div}(\langle \rho_v \rangle \langle \vec{V}_v \rangle^g) = \dot{m}_v \quad (4)$$

$$\frac{\partial \langle \rho_a \rangle}{\partial \tau} + \text{div}(\langle \rho_a \rangle \langle \vec{V}_a \rangle^g) = 0 \quad (5)$$

Where  $\langle \rho_l \rangle = \langle \rho_l \rangle^l S_l \phi$ ,  $\langle \rho_v \rangle = \langle \rho_v \rangle^g (1 - S_l) \phi$ ,

$\langle \rho_a \rangle = \langle \rho_a \rangle^g (1 - S_l) \phi$

Darcy's law is expressed as following:

$$\langle \vec{V}_i \rangle^i = \langle \vec{V}_s \rangle^s - \frac{1}{S_i \phi} \frac{k k_i}{\mu_i} \overline{\text{grad}} \langle P_i \rangle^i \quad (i = l, g) \quad (6)$$

Intrinsic velocity of both vapour and dry air phases could be written as following:

$$\langle \vec{V}_i \rangle^g = \langle \vec{V}_g \rangle^g + \langle \vec{u}_i \rangle^g \quad (i = a, v) \quad (7)$$

Where  $\langle \vec{V}_g \rangle^g$  is the barycentric velocity of gas phase and  $\langle \vec{u}_i \rangle^g$  is the diffusion velocity of vapour and dry air into gaseous phase.

To express the diffusion velocity, the Fick's law is used:

$$\langle \rho_v \rangle \langle \vec{u}_v \rangle^g = -\langle \rho_a \rangle \langle \vec{u}_a \rangle^g = -\langle \rho_g \rangle^g D_g \overline{\text{grad}} \frac{\langle \rho_v \rangle^g}{\langle \rho_g \rangle^g} \quad (8)$$

The liquid pressure is defined as:

$$\langle P_l \rangle^l = \langle P_g \rangle^g - \langle P_c \rangle \quad (9)$$

Final form of constitute equations model is written as follows:

The mass balance equation of water in both liquid and vapour form is:

$$\begin{aligned} & \frac{\partial (\langle \rho_l \rangle^l S_l + \langle \rho_v \rangle^g S_g) \phi}{\partial \tau} + \text{div} \left( (\langle \rho_l \rangle^l S_l + \langle \rho_v \rangle^g (1 - S_l)) \phi \langle \vec{V}_s \rangle^s \right) \\ & + \text{div} \left( -\langle \rho_l \rangle^l \frac{k k_l}{\mu_l} \overline{\text{grad}} (\langle P_g \rangle^g - \langle P_c \rangle) \right) + \text{div} \left( -\langle \rho_v \rangle^g \frac{k k_g}{\mu_g} \overline{\text{grad}} \langle P_g \rangle^g \right) \\ & + \text{div} \left( -\langle \rho_g \rangle^g D_g \overline{\text{grad}} \frac{\langle \rho_v \rangle^g}{\langle \rho_g \rangle^g} \right) \\ & = 0 \end{aligned} \quad (10)$$

The dry air mass conservation equation may be written as:

$$\begin{aligned} & \frac{\partial (\langle \rho_a \rangle^g (1 - S_l) \phi)}{\partial \tau} + \text{div}(\langle \rho_a \rangle^g (1 - S_l) \phi \langle \vec{V}_s \rangle^s) \\ & + \text{div} \left( -\langle \rho_a \rangle^g \frac{k k_g}{\mu_g} \overline{\text{grad}} \langle P_g \rangle^g \right) + \text{div} \left( \langle \rho_g \rangle^g D_g \overline{\text{grad}} \frac{\langle \rho_v \rangle^g}{\langle \rho_g \rangle^g} \right) \\ & = 0 \end{aligned} \quad (11)$$

Summing mass balance equation of liquid, vapour and solid phases, we obtain the following expression:

$$\begin{aligned}
& \frac{\partial(\langle\rho_l\rangle^l S_l + \langle\rho_v\rangle^g S_g - 1)\phi}{\partial t} + \operatorname{div}\left(\langle\rho_l\rangle^l S_l + \langle\rho_v\rangle^g (1 - S_l) - 1\right)\phi \langle\vec{V}_s\rangle^s \\
& + \operatorname{div}\left(\langle\vec{V}_s\rangle^s\right) + \operatorname{div}\left(-\langle\rho_l\rangle^l \frac{kk_l}{\mu_l} \overrightarrow{\operatorname{grad}}(\langle P_g\rangle^g - \langle P_c\rangle)\right) \\
& + \operatorname{div}\left(-\langle\rho_v\rangle^g \frac{kk_g}{\mu_g} \overrightarrow{\operatorname{grad}}\langle P_g\rangle^g\right) + \operatorname{div}\left(-\langle\rho_g\rangle^g D_g \overrightarrow{\operatorname{grad}}\frac{\langle\rho_v\rangle^g}{\langle\rho_g\rangle^g}\right) \\
& = 0
\end{aligned} \tag{12}$$

## 2.2 Energy conservation equation

The macroscopic energy balance equation is:

$$\begin{aligned}
& \rho C_p \frac{\partial T}{\partial t} + \left(\langle\rho C_p\rangle_s \langle\vec{V}_s\rangle + \langle\rho C_p\rangle_l \langle\vec{V}_l\rangle + \langle\rho C_p\rangle_a \langle\vec{V}_a\rangle + \langle\rho C_p\rangle_v \langle\vec{V}_v\rangle\right) \overrightarrow{\operatorname{grad}}T + \\
& \operatorname{div}\left(-\lambda_{eff} \overrightarrow{\operatorname{grad}}T\right) = -h_v \dot{m}_v
\end{aligned} \tag{13}$$

Where the rate of water vaporization per unit volume appearing in equation (13) takes the form:

$$-\dot{m}_v = \frac{\partial\langle\rho_l\rangle^l S_l \phi}{\partial t} + \operatorname{div}\left(\langle\rho_l\rangle^l S_l \phi \langle\vec{V}_l\rangle^l\right) + \operatorname{div}\left(-\langle\rho_l\rangle^l \frac{kk_l}{\mu_l} \overrightarrow{\operatorname{grad}}(\langle P_g\rangle^g - \langle P_c\rangle)\right) \tag{14}$$

The heat capacity is expressed as:

$$\rho C_p = \langle\rho_s\rangle^s (1 - \phi) C_{ps} + \langle\rho_l\rangle^l S_l \phi C_{pl} + \langle\rho_v\rangle^g (1 - S_l) \phi C_{pv} + \langle\rho_a\rangle^a (1 - S_l) \phi C_{pa} \tag{15}$$

## 2.3 Momentum conservation equation

The mechanical equilibrium equation, with the hypothesis of elastic behaviour of material:

$$\operatorname{div}\left(\lambda \operatorname{tr}(\bar{\varepsilon}) \bar{I} + 2\mu \bar{\varepsilon} - \langle P_g\rangle^g \bar{I} + S_l \langle P_c\rangle \bar{I}\right) = 0 \tag{16}$$

The total strain of a dried media could be written as:

$$\varepsilon_{ij} = \frac{1}{2}(u_{i,j} + u_{j,i}) \tag{17}$$

## 2.4 Boundary condition

The boundary condition associated with equations (10), (11), (12), (13) and (16):

At the drying surface:

$$\left(\langle\rho_l\rangle \langle\vec{V}_l\rangle^l + \langle\rho_v\rangle \langle\vec{V}_v\rangle^g\right) \cdot \vec{n} = F_m \tag{18}$$

$$\langle P_g\rangle^g = P_{atm} \tag{19}$$

$$\left(-\lambda_{eff} \overrightarrow{\operatorname{grad}}T\right) \cdot \vec{n} = -h_v F_m + h(T_s - T_\infty) \tag{20}$$

$$\bar{\sigma} \cdot \vec{n} = 0 \tag{21}$$

At the symmetric surface:

$$\left(\langle\rho_l\rangle \langle\vec{V}_l\rangle^l + \langle\rho_v\rangle \langle\vec{V}_v\rangle^g\right) \cdot \vec{n} = 0 \tag{22}$$

$$(-\lambda_{eff} \overline{\text{grad} T}) \cdot \vec{n} = -0 \quad (23)$$

$$\overline{\text{grad}(P_g)^g} \cdot \vec{n} = -0 \quad (24)$$

$$\vec{\sigma} \cdot \vec{n} = 0 \quad (25)$$

$$\vec{u} \cdot \vec{n} = 0 \quad (26)$$

### 3 Results and discussion

The equations (10), (11), (12), (13) and (16), associated with boundary conditions, were resolved to determine the five variables of the problem  $\mathbf{S}_1$ ,  $\phi$ ,  $(P_g)^g$ ,  $T$  and  $(\vec{V}_s)^s$ . The model is implemented in a finite element solver. The Arbitrary Lagrange-Eulerian (ALE) formulation was used to solve the problem with moving boundaries; this allowed consideration of a drying process of a shrinking body as is the case of the present study.

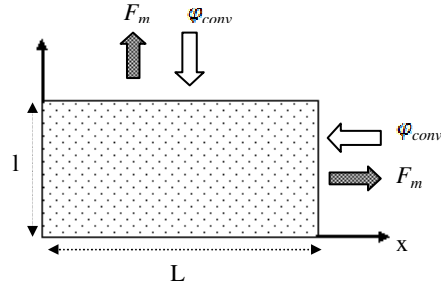


**Fig. 1.** Schematic representation of the bi-dimensional configuration

The physical and mechanical properties of the material injected in the model are summarized in table 1.

In order to visualise the effect of drying of hardened cement paste sample at constant and variable conditions, the drying kinetics and induced normal stresses were determined. The changes of air parameters was applied periodically at the end of the constant drying rate period (in our case at time=500s) with period equal to 800s. Figure 2 shows the time evolution of average moisture content, temperature and gas pressure at the centre for stationary drying at 80°C and 5% of relative humidity and for three cases of non stationary drying: drying with periodical variation of air temperature between 80°C and 30°C, drying with periodical variation of air relative humidity between 5% and 50% and combined periodical variation of air temperature and relative humidity.

**Table 1.** Input parameters

Parameter	Expression
Sorption curve	$W = \frac{w_m K C a_w}{(1 - K a_w)(1 - K a_w + C K a_w)}$ $K = 0.93$ $C = 43$ $w_m = 0.0025$
Relative permeability[11]	Liquid permeability $k_l = S_i^p (1 - (1 - S_i^{1/m})^m)^2$ Gas permeability $k_g = (1 - S_i)^p (1 - S_i^{1/m})^{2m}$ $m = 0.307$ $p = 0.5$
Capillary pressure[10]	$\alpha (S_i^{-1/m} - 1)^{1/n}$ $\alpha = 41.7 \cdot 10^6$ $n = 1.89$ $m = 1 - 1/n$
Water vapour diffusion[10]	$D_{eff} = D_{va}^0 \left( \frac{P_{atm}}{P_g} \right) \left( \frac{T}{T_0} \right)^{1.88} f(S_i, \phi)$ $D_{va}^0 = 2.17 \cdot 10^{-5}$ $f(S_i, \phi) = \phi^{2.74} (1 - S_i)^{4.2}$
Elastic modulus	$E = 27 GPa$
Poisson coefficient	$\nu = 0.3$
Intrinsic solid density	$\langle \rho_s \rangle^s = 2000 \text{ kg/m}^3$
Effective thermal conductivity	$\lambda_{eff} = 1.5 \text{ Wm}^{-1}\text{K}^{-1}$
Initial conditions	$S_{i0} = 0.95$ $\phi_0 = 0.3$ $\langle P_g \rangle_0^s = 101325 Pa$ $T_0 = 293 K$ $\langle \vec{V}_s \rangle_0^s = 0 \text{ m/s}$ $L = 0.02m \quad l = 0.01m$

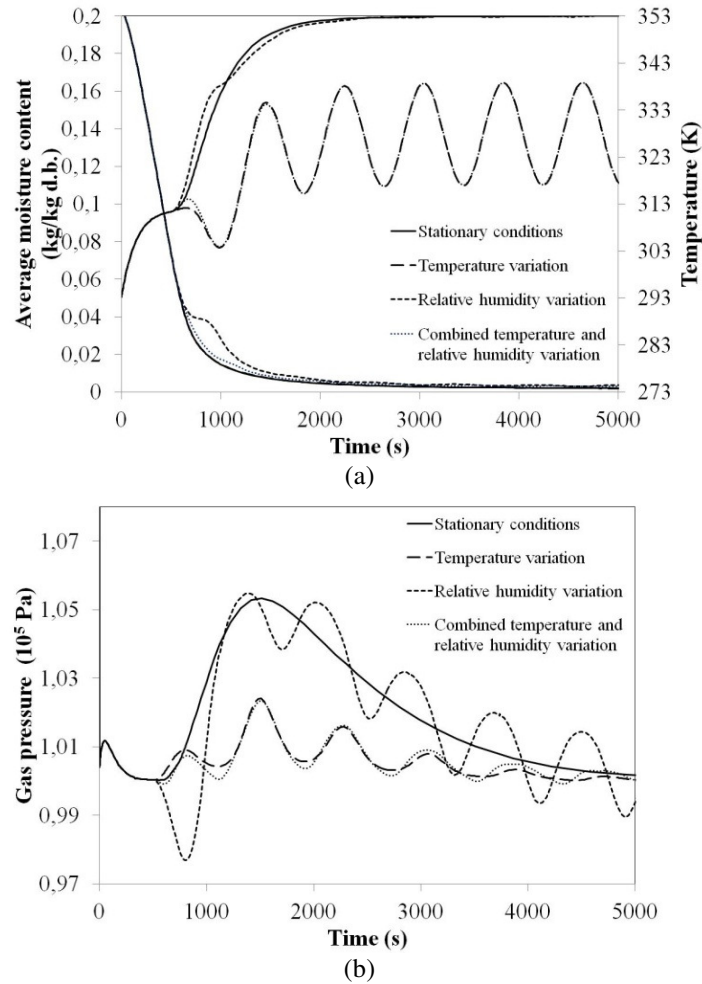


**Fig. 2.** Drying kinetics of hardened cement paste sample: (a) time evolution of average moisture content and temperature (b) time evolution of gas pressure at the centre

Moisture content starts from an initial value equal to 0.2 kg/kg d.b. that corresponds to initial saturation  $S_{i0} = 0.95$  and initial porosity  $\phi_0 = 0.3$ . At the beginning of drying at constant conditions, sample temperature increases until to reach the wet bulb temperature. A constant drying rate phase was noticed, corresponding to a linear diminution of moisture content. Then, the media enters the hygroscopic range and free water was totally evaporated that develops gas pressure inside the porous media up to  $1.05 \cdot 10^5$  Pa at 1500s. When humidity distribution becomes more homogenous, the moisture content approaches to its equilibrium value and the gas pressure goes down to the atmospheric pressure. Note that the influence of periodical changes of air temperature on moisture content is insignificant. However, it has a considerable effect on sample temperature and gas pressure. This is

manifested by the formation of great oscillations and the reduction of the peak of gas pressure to  $1.02 \cdot 10^5$  Pa. It is seen that drying at variable temperature accompanied with humidity variation slows down the drying process. Sample temperature and gas pressure curves are similar to drying curves at variable temperature.

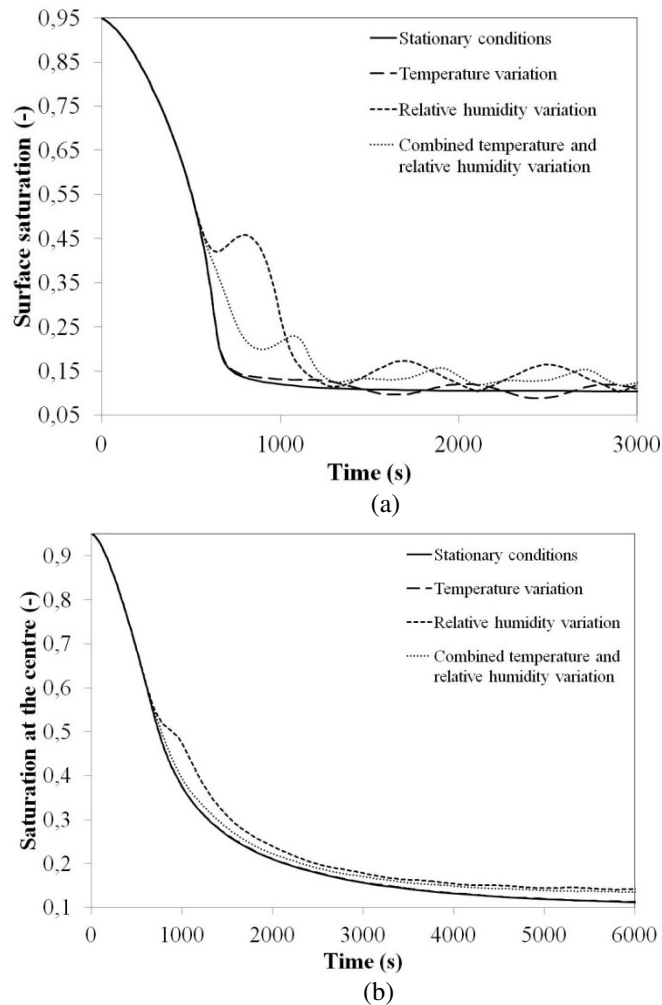


**Fig. 3.** Time evolution of saturation of hardened cement paste sample: (a) at the surface (b) at the centre

On the other hand, the changes of relative humidity cause immediate reduction of drying rate and insignificant oscillations of temperature. The increase of relative humidity causes direct falling of gas pressure. Figure 2 (b) shows that the peak of gas pressure reached in stationary conditions is not influenced by the



changes of air humidity. The time of drying is the same for both constant and variable conditions.

In figure 3, the effect of drying conditions on the time evolution of saturation at the surface and within the material was presented. It is noticed a significant consequence of periodical changes of air conditions on surface saturation profile. The air relative humidity decrease induces an instantaneous growth of surface saturation. Compared to stationary drying these changes slow down the drying rate but do not affect the equilibrium value of surface saturation ( $S_{1\epsilon q} = 0.1$ ). Following the development of saturation at the centre, curves indicate a very small swings and a slight increase of saturation in the cases of relative humidity variation and temperature accompanied with relative humidity variation.

Figure 4 presents the normal stresses development at the surface in P(0,0.01) during stationary and alternating drying. It is clearly seen, during drying at constant conditions, the normal stresses increase with time and achieve a maximum value just after the end of the constant drying rate. At this maximum the risk of material fissure is the top. Compared to drying with periodical diminution of air temperature, the maximum normal stresses is slightly reduced from 6.14 MPa (at 740s) for constant conditions to 5.9 MPa. Drying with periodical changes of relative humidity causes a more decrease of stresses to 5.14 MPa. Curves in figure 4 allow us to affirm that the lowest normal stresses are obtained in drying with both air temperature and relative humidity changes. The maximum value is reduced to 3.88 MPa. Kowalski and Pawlowski [7,8] investigated experimentally the stationary and intermittent drying (with periodical variation of temperature and relative humidity) of wood and kaolin-clay. It was demonstrated that the best quality is achieved in drying with changeable relative humidity and the worst is obtained in drying at stationary conditions. Thus, our results are in good agreement with this similar study.

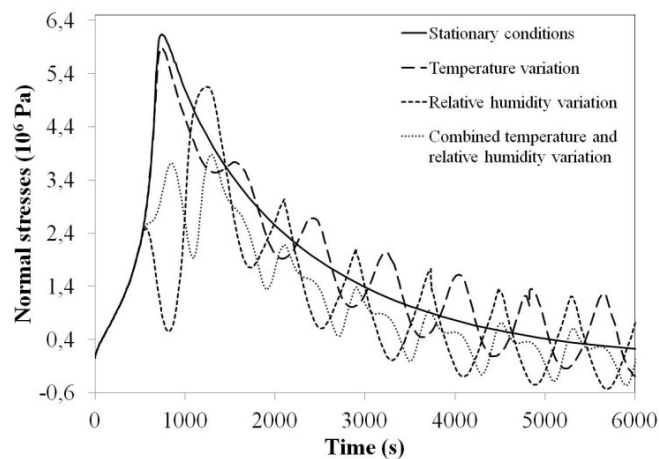


Fig. 4. Time evolution of normal stresses of hardened cement paste sample

## 4 Conclusions

A multiphase model was developed to describe the hydro-thermo-mechanical behaviour of hardened cement paste during drying. The aim of this analysis is to examine the advantages of non stationary drying. The results allow us to state that drying with periodical changes of air conditions reduces generated stresses without extending drying time. The combination of air temperature and relative humidity variation during drying assures the smallest development of normal stresses. Consequently, it can be confirmed that drying in this case guarantee the best quality of hardened cement paste.

## Nomenclature

$C_p$	Heat capacity ( $J\ kg^{-1}\ K^{-1}$ )
$D_{eff}$	Effective diffusion coefficient ( $m^2\ s^{-1}$ )
$E$	Young modulus (Pa)
$F_m$	Mass flux ( $kg\ m^{-2}\ s^{-1}$ )
$h$	Heat transfer coefficient ( $W\ m^{-2}$ )
$h_m$	Mass transfer coefficient ( $m\ s^{-2}$ )
$h_v$	Evaporation latent heat ( $J\ kg^{-1}$ )
$k$	Intrinsic permeability ( $m^2$ )
$k_i$	Relative permeability
$n$	Normal
$P$	Pressure (Pa)
$P_c$	Capillary pressure (Pa)
$S_l$	Water saturation
$T$	Temperature
$t$	Time (s)
$V$	Velocity ( $m\ s^{-1}$ )
$w$	Moisture content (dry basis)
$\nu$	Poisson coefficient
$\mu$	Dynamic viscosity ( $kg\ m^{-1}\ s^{-1}$ )
$\phi$	Porosity
$\varepsilon$	Strain
$\sigma$	Stress (Pa)
$\rho$	Density ( $kg\ m^{-3}$ )
$\lambda_{eff}$	Effective thermal conductivity ( $W\ m^{-1}\ K^{-1}$ )
$\varphi_{conv}$	Convective heat flux ( $W\ m^{-2}$ )

*Mathematical symbols*

$\underline{\xi}$	Tensorial symbol
$\vec{\xi}$	Vector symbol
$\langle \xi_i \rangle$	Apparent average of i phase
$\langle \xi_i \rangle^i$	Intrinsic average of i phase

*Subscripts and superscripts*

a	Dry air phase
g	Gaseous phase
l	Liquid phase
s	Solid phase
v	Vapour phase

**References**

1. N. Burlion , I. Yurtdas, F. Skoczylas, “Comportement mécanique et séchage de matériaux à matrice cimentaire“, Revue française de génie civil. Vol 7 – n° 2/2003, 145 à 165, 2011.
2. F. Benboudjema, F. Meftah, J. M. Torrenti, Interaction between drying, shrinkage, creep and cracking Phenomena in Concrete, Engineering Structures, 27, 239-250, 2005.
3. S. Withaker, “Flow in porous media III: deformable media”, Transport Porous Media, 1, 127-154, 1986.
4. B.A.. Schrefler, “Mechanics and thermodynamics of saturated/unsaturated porous materials and quantitative solutions”, Appl Mech Rev, 55 (4), 2002.
5. P. Rattanadecho, W. Pakdee, and J. Stakulcharoen, “Analysis of multiphase flow and heat transfer: Pressure buildup in an unsaturated porous slab exposed to hot gas”, Drying Technology, 26, 39–53, 2008.
6. Z. X. Gong, B. Song , A.S. Mujumdar, “Numerical simulation of drying of refractory concrete”, drying technology, 9(2), 479-500, 1991.
7. S.J. Kowalski, A. Pawlowski, “Drying of wood air of variable parameters”, Chemical Engineering Science, 31, 135-147, 2010.
8. S.J. Kowalski, A. Pawlowski, “Intermittent drying of initially saturated porous materials”, Chemical Engineering Science, 66, 1893-1905, 2011.
9. S.J. Kowalski, J. Szadzinska, “Non-stationary drying of ceramic-like materials controlled through acoustic emission method”, Heat and mass transfer, 48, 2023-2032, 2012.
10. M.D. Nguyen, “ Modélisation du couplage entre hydratation et dessiccation des matériaux cimentaires à l’issue du décoffrage-Etude de la dégradation des propriétés de transfert “, thesis, Ecole nationale des ponts et chaussées, 2009.
11. V. Baroghel-Bouny, M. Thiery, F. Barberon, O. Coussy, G. Villain, “Assessment of transport properties of cementitious materials”, Transfert dans les géomatériaux, 671 – 696, 2011.